

## Chapter 3

# Concepts in Mesoscopic Physics

### 3.1 Drude Conductivity, Einstein Relation

When an electric field  $E$  is applied on a diffusive conductor, scattering randomizes the momenta of electrons on a length scale of the mean free path  $\ell$ , but a drift velocity  $v_d$  results as well. Electrons are accelerated for a time  $\tau_m$ , the momentum relaxation time. Then they are scattered and are assumed to lose their momentum. In equilibrium, the rate at which electrons receive momentum from the external field is exactly equal to the rate at which they lose momentum:

$$\left[ \frac{dp}{dt} \right]_{\text{scattering}} = \left[ \frac{dp}{dt} \right]_{\text{field}}, \quad (3.1)$$

giving for the drift velocity:

$$\frac{m^* v_d}{\tau_m} = eE, \quad \Rightarrow \quad v_d = \frac{e\tau_m}{m^*} E. \quad (3.2)$$

The mobility  $\mu$  is defined via:

$$v_d = \mu E, \quad \Rightarrow \quad \mu = \frac{e\tau_m}{m^*} \quad (3.3)$$

Via the current density  $j = nev_d = \sigma E$  one obtains the *Drude conductivity*,

$$\sigma = en\mu = \frac{ne^2\tau_m}{m^*} \quad (3.4)$$

the classical expression for conductivity in a diffusive metal. Here, current is carried by drift of *all* the electrons. However, for a degenerate Fermi-gas  $kT \ll E_F$ , we have seen that the Fermi sea is filled up to Fermi wave-vector  $k_F$  and Fermi energy  $E_F$ :

$$k_F = \sqrt{\frac{4\pi n}{g_s g_v}} \Big|_{g_s=2, g_v=1} = \sqrt{2\pi n}, \quad E_F = \frac{\hbar^2 k_F^2}{2m^*} = \frac{\pi \hbar^2}{m^*} n \quad (3.5)$$

with  $g_s$  the spin degeneracy (in *GaAs*, at  $B = 0$ ,  $g_s = 2$ ), and  $g_v$  the valley degeneracy (in *GaAs*,  $g_v = 1$ ). One finds that nonzero current is carried only by electrons within some  $kT$  around the Fermi energy, since at lower energies into the filled Fermi sea, right moving states  $+k$  exactly cancel left moving states  $-k$ . To understand the conduction properties,

one does not need to worry about the dynamics of all the electrons in the Fermi sea, it is sufficient to consider electrons close to the Fermi surface, where electrons move with the Fermi velocity

$$v_F = \frac{\hbar k_F}{m^*}. \quad (3.6)$$

Current is then carried by only a small fraction of electrons:  $j = e(nv_d/v_F)v_F$ . Scattering still occurs with an average time  $\tau_m$ , giving a mean free path

$$\ell = v_F \tau_m \quad (3.7)$$

Using Eq. 3.5 and the above expression for  $\ell$ , the conductivity can then be written in the following convenient form:

$$\sigma = g_s g_v \frac{e^2}{h} \frac{k_F \ell}{2} = \frac{2e^2}{h} \frac{k_F \ell}{2}, \quad (3.8)$$

i.e. the conductivity is expressed by the ratio of mean free path  $\ell$  and the Fermi wavelength  $\lambda_F = 2\pi/k_F$ . In metals,  $k_F \ell$  is much greater than one, and  $e^2/h \sim 25.812 \text{ k}\Omega$ . Recalling our expression for the 2D density of states

$$\rho_{DOS} = \frac{g_s g_v m^*}{2\pi \hbar^2} = \frac{m^*}{\pi \hbar^2} \quad (3.9)$$

and introducing the diffusion constant

$$D = \frac{1}{2} v_F^2 \tau_m = \frac{1}{2} v_F \ell \quad (3.10)$$

the conductivity can also be written as

$$\sigma = e^2 \rho_{DOS}(E) D, \quad (3.11)$$

expressing the conductivity in terms of density of states at the Fermi level (*Einstein relation*), which in 2D is independent of energy since the density of states is independent of energy. It is worth noting that in 2D—unlike in 3D or 1D—the resistivity  $\rho$ , a material parameter independent of sample shape and size, and the resistance  $R$  of a given sample have the same units (Ohms,  $\Omega$ ) and are related via a dimensionless quantity  $L/W$ , the number of length  $L$  and width  $W$  of a sample:

$$R = \rho \frac{L}{W} = \rho_{\square} \frac{L}{W}, \quad (3.12)$$

where we introduced the resistance or resistivity per square  $\rho_{\square} = \rho$ . The resistance of a sample can therefore conveniently be calculated by counting the number of squares that fit into the sample region since the resistance  $R$  of a square is independent of the size of the square (again, this is only applicable in 2D).

## 3.2 Mesoscopic Time and Length Scales

There are several important length and time scales that commonly appear in mesoscopic physics. Here is a short description:

### 3.2.1 Femi wavelength $\lambda_F$

As we have seen, at low temperatures  $kT \ll E_F$ , current is carried by electrons a few  $kT$  around  $E_F$ . The relevant length associated with these electrons is the Fermi wavelength

$$\lambda_F = 2\pi/k_F = \sqrt{2\pi/n} \quad (3.13)$$

which depends only on the carrier density  $n$ . Typically,  $n \sim 2 \times 10^{11} \text{ cm}^{-2} = 2 \times 10^{15} \text{ m}^{-2}$ , giving a Fermi energy  $E_F \sim 7 \text{ meV}$  (using the effective mass  $m^* = 0.067m_e$ ) and  $\lambda_F \sim 56 \text{ nm}$ . Electrons below the Fermi energy have correspondingly longer wavelengths. Typical Fermi velocities are  $v_F = \hbar k_F/m^* = 195'000 \text{ m/s}$ .

### 3.2.2 Mean free path $\ell$

As we have seen, electrons get scattered due to phonons, impurities, interface effects etc, resulting in a mean free path

$$\ell = v_F \tau_m = v_F \mu \frac{m^*}{e} \quad (3.14)$$

using  $\mu = \tau_m e/m^*$ . Since the mobility is defined via the resistivity, it is a measure of backscattering, rather than small angle scattering. For a mobility of  $\mu = 100 \text{ m}^2/(\text{Vs}) = 1'000'000 \text{ cm}^2/(\text{Vs})$ , a backscattering time of  $\tau_m = 38 \text{ ps}$ , a mean free path of  $\ell = 7.4 \mu\text{m}$  and a diffusion constant of  $D = 0.72 \text{ m}^2/\text{s}$  result. A device of size  $L$  is called *ballistic* if  $\ell \gg L$  and *diffusive* if  $\ell \ll L$ .

### 3.2.3 Phase coherence time $\tau_\varphi$

In a quantum mechanical (or at least semi-classical) description, electrons carry not only momentum, energy and spin but also a phase. For example, for a plane wave  $e^{ik_F x + i\varphi}$  the phase  $\varphi$  is some well defined value (often chosen  $\varphi = 0$  for convenience). When waves are interfered, for example in the paradigmatic double slit experiment, the resulting interference pattern is  $|A_1 + A_2|^2 \sim \text{Re} \exp(ik_F(L_1 - L_2) + i(\varphi_1 - \varphi_2))$ , i.e. the relative phase  $\varphi_1 - \varphi_2$  becomes relevant. If in some way  $\varphi_{1,2}$  are randomized efficiently, then the time-averaged interference will be zero, due to the loss of phase coherence. The phase coherence time  $\tau_\varphi$  is the average time by which any such interference term is suppressed by  $e^{-1}$ , and by  $\exp(-t/\tau_\varphi)$  after a time  $t$ . In mesoscopic physics, quantum interference effects are often of central importance, making  $\tau_\varphi$  an essential time scale of the system.

Scattering on rigid impurities might add an additional phase to an electron in, say, one arm of an interferometer, but, since it is static, it will always be the same phase throughout the experment, still leading to a stationary, unsuppressed interference pattern (though shifted). Therefore, rigid scatterers do not cause decoherence. On the other hand, dynamic or fluctuating scatterers lead to a time dependent  $\varphi(t)$ . If the timescale of the measurement is much longer than the coherence time  $\tau_\varphi$  over which  $\varphi(t)$  is randomized:

$\langle \varphi \rangle_t = \int_0^t \varphi(\tau) d\tau \sim 0$ , the interference term  $\langle \exp(i\varphi(\tau)) \rangle_t \sim \exp(-t/\tau_\varphi)$  is exponentially suppressed due to loss of phase coherence.

The nature of decoherence can be complicated, involving various dynamic scattering mechanisms with different effectiveness that might depend on parameters such as temperature and magnetic field: lattice vibrations (electron-phonon scattering), scattering off the Coulomb potential created by other electrons (electron-electron interactions) and impurities with an internal degree of freedom (for example spin), to name just a few. At low temperatures ( $T < 1$  K), often phonons are frozen out (though they might still be emitted) and electron-electron interactions are the dominant decoherence mechanism (assuming negligible impurity scattering). Within electron-electron scattering, one distinguishes between scattering with large energy exchange, where phase coherence can be lost in one event (often weak at low temperature due to lack of phase space), and the Nyquist mechanism, where phase coherence is lost only after many quasi-elastic scattering events.

In ballistic samples, the associated coherence length is trivially given by

$$L_\varphi = v_F \tau_\varphi, \quad (3.15)$$

while in diffusive samples

$$L_\varphi = \sqrt{D\tau_\varphi}. \quad (3.16)$$

A *quasi one-dimensional* sample has one dimension  $L$  much smaller than the relevant coherence length:  $L \ll L_\varphi$ .

### 3.2.4 Thermal length $L_T$

At finite temperature, electrons within a few  $kT$  around  $E_F$  contribute to transport. Starting at a common location with momentum in the same direction, an electron at Fermi energy  $E_F$  will get out of phase by one radian with an electron at  $E_F + kT$  after traveling the *thermal length*  $L_T$  (because the two wavelengths are slightly different). In a ballistic sample, this length is easily calculated using  $(k(E_F + kT) - k(E_F))x = 1$  and the dispersion relation  $k(E) = \sqrt{2m^*E}/\hbar$ . Assuming  $E_F \gg kT$ , one finds

$$L_T = \frac{\hbar v_F}{kT}, \quad (3.17)$$

corresponding to a *thermal time*  $\tau_T = \hbar/(kT)$ , which we could have also guessed from a consideration using the time-domain Heisenberg uncertainty relation  $\Delta t \cdot \Delta E \geq \hbar$  with  $\Delta E = kT$ . With similar sample parameters as before at  $T = 0.1$  K, one obtains  $L_T \sim 15 \mu\text{m}$ , which is larger than the calculated mean free path, rendering the ballistic approach incorrect. Maybe a diffusive approach would be more appropriate. In a diffusive sample, the thermal time  $\tau_T$  will be used to diffuse through the sample, giving a diffusive thermal length

$$L_T = \sqrt{\frac{\hbar D}{kT}}, \quad (3.18)$$

corresponding to  $L_T \sim 7.4 \mu\text{m}$  (for  $T = 0.1$  K). This is equal to the mean free path, so neither a purely diffusive nor purely ballistic treatment appears appropriate here.

### 3.2.5 Interaction parameter $r_S$

We have treated the 2D electron gas so far as an ideal, non-interacting Fermi gas. One way to quantify whether this is an appropriate approximation is the ratio between average (unscreened) Coulomb energy and kinetic energy of electrons in the gas.

$$r_S = \frac{e^2}{4\pi\epsilon_0\epsilon r} \div E_F = \frac{e^2 m^*}{\epsilon\epsilon_0 h^2} \frac{1}{\sqrt{n}} \sim 0.7 \quad (3.19)$$

where the average spacing between electrons is taken as  $r = \sqrt{1/n} \sim 22$  nm and  $E_F = \hbar^2 k_F^2 / (2m^*)$ . The non-interacting approximation is exact in the limit  $r_s \rightarrow 0$  and is not valid for  $r_s \gtrsim 1$ , called the strongly interacting regime. The above expression might be corrected somewhat towards smaller  $r_s$  due to screening, but it is obvious that particularly for low carrier densities the strongly interacting regime is reached in *GaAs* 2D electron gases.

TABLE I Electronic properties of the 2DEG in GaAs-AlGaAs heterostructures and Si inversion layers.

		GaAs(100)	Si(100)	Units
Effective Mass	$m$	0.067	0.19	$m_e = 9.1 \times 10^{-28}$ g
Spin Degeneracy	$g_s$	2	2	
Valley Degeneracy	$g_v$	1	2	
Dielectric Constant	$\epsilon$	13.1	11.9	$\epsilon_0 = 8.9 \times 10^{-12}$ Fm <sup>-1</sup>
Density of States	$\rho(E) = g_s g_v (m/2\pi\hbar^2)$	0.28	1.59	$10^{11}$ cm <sup>-2</sup> meV <sup>-1</sup>
Electronic Sheet Density <sup>a</sup>	$n_s$	4	1–10	$10^{11}$ cm <sup>-2</sup>
Fermi Wave Vector	$k_F = (4\pi n_s / g_s g_v)^{1/2}$	1.58	0.56–1.77	$10^6$ cm <sup>-1</sup>
Fermi Velocity	$v_F = \hbar k_F / m$	2.7	0.34–1.1	$10^7$ cm/s
Fermi Energy	$E_F = (\hbar k_F)^2 / 2m$	14	0.63–6.3	meV
Electron Mobility <sup>a</sup>	$\mu_e$	$10^4 - 10^6$	$10^4$	cm <sup>2</sup> /Vs
Scattering Time	$\tau = m\mu_e/e$	0.38–38	1.1	ps
Diffusion Constant	$D = v_F^2 \tau / 2$	140–14000	6.4–64	cm <sup>2</sup> /s
Resistivity	$\rho = (n_s e \mu_e)^{-1}$	1.6–0.016	6.3–0.63	k $\Omega$
Fermi Wavelength	$\lambda_F = 2\pi/k_F$	40	112–35	nm
Mean Free Path	$l = v_F \tau$	$10^2 - 10^4$	37–118	nm
Phase Coherence Length <sup>b</sup>	$l_\phi = (D\tau_\phi)^{1/2}$	200–...	40–400	nm(T/K) <sup>-1/2</sup>
Thermal Length	$l_T = (\hbar D/k_B T)^{1/2}$	330–3300	70–220	nm(T/K) <sup>-1/2</sup>
Cyclotron Radius	$l_{\text{cycl}} = \hbar k_F / eB$	100	37–116	nm(B/T) <sup>-1</sup>
Magnetic Length	$l_m = (\hbar/eB)^{1/2}$	26	26	nm(B/T) <sup>-1/2</sup>
	$k_F l$	15.8–1580	2.1–21	
	$\omega_c \tau$	1–100	1	(B/T)
	$E_F / \hbar \omega_c$	7.9	1–10	(B/T) <sup>-1</sup>

<sup>a</sup>A typical (fixed) density value is taken for GaAs-AlGaAs heterostructures, and a typical range of values in the metallic conduction regime for Si MOSFET's. For the mobility, a range of representative values is listed for GaAs-AlGaAs heterostructures, and a typical "good" value for Si MOSFET's. The variation in the other quantities reflects that in  $n_s$  and  $\mu_e$ .

<sup>b</sup>Rough estimate of the phase coherence length, based on weak localization experiments in laterally confined heterostructures<sup>23,24,25,26,27</sup> and Si MOSFET's.<sup>28,29</sup> The stated  $T^{-1/2}$  temperature dependence should be regarded as an indication only, since a simple power law dependence is not always found (see, for example, Refs.<sup>30</sup> and<sup>25</sup>). For high-mobility GaAs-AlGaAs heterostructures the phase coherence length is not known, but is presumably<sup>31</sup> comparable to the (elastic) mean free path  $l$ .

### 3.2.6 Magnetic Length $\ell_B$

In many instances involving magnetic fields, the area  $A = \hbar/(eB)$  through which one flux quantum is threaded is of relevance, giving a corresponding length scale

$$\ell_B = \sqrt{\frac{\hbar}{eB}}. \quad (3.20)$$

This is also the spatial extent of wavefunctions in a magnetic field, of importance in the quantum Hall effect.

## 3.3 Classical Hall Effect

It is easy to include a magnetic field  $B$  perpendicular to the 2DEG in the classical resistivity consideration, using the equilibrium relaxation condition:

$$\left[ \frac{dp}{dt} \right]_{\text{scattering}} = \left[ \frac{dp}{dt} \right]_{\text{field}}, \quad (3.21)$$

which can be written out as

$$\frac{m^* v_d}{\tau_m} = e [E + v_d \wedge B], \quad (3.22)$$

or, using a matrix notation:

$$\begin{pmatrix} \frac{m^*}{e\tau_m} & -B \\ +B & \frac{m^*}{e\tau_m} \end{pmatrix} \begin{pmatrix} v_x \\ v_y \end{pmatrix} = \begin{pmatrix} E_x \\ E_y \end{pmatrix}, \quad (3.23)$$

where  $v_x$  and  $v_y$  are the x- and y- components of the drift velocity and  $E_x$  and  $E_y$  are the x- and y- components of the electric field. Using  $j = ev_d n$ ,  $\sigma = en\mu$  and  $\mu = e\tau_m/m^*$ , one obtains the resistivity tensor:

$$\begin{pmatrix} E_x \\ E_y \end{pmatrix} = \sigma^{-1} \begin{pmatrix} 1 & -\mu B \\ +\mu B & 1 \end{pmatrix} \begin{pmatrix} j_x \\ j_y \end{pmatrix} = \begin{pmatrix} \rho_{xx} & \rho_{xy} \\ \rho_{yx} & \rho_{yy} \end{pmatrix} \begin{pmatrix} j_x \\ j_y \end{pmatrix}. \quad (3.24)$$

One then finds for the longitudinal resistivity  $\rho_{xx}$  and transverse resistivity  $\rho_{xy}$ :

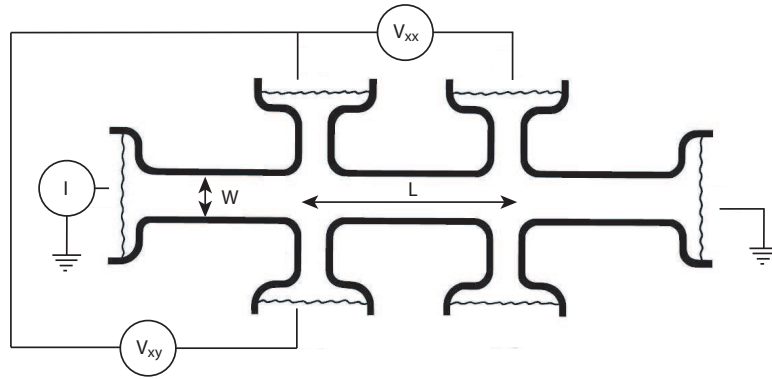
$$\rho_{xx} = \sigma^{-1}, \quad \rho_{xy} = -\rho_{yx} = -\frac{B}{en}. \quad (3.25)$$

In a Hall bar geometry of width  $W$  and length  $L$ , with a current  $I_x = Wj_x$  driven in the x-direction ( $j_y = 0$ ),  $E_x = \rho_{xx}j_x$  and  $E_y = \rho_{yx}j_x$  results. Using  $V_x = LE_x$ ,  $V_y = V_H = E_yW$  one gets:

$$V_x = R_{xx}I_x, \quad \text{with} \quad R_{xx} = \frac{L}{W}\rho_{xx} \quad (3.26)$$

$$V_H = V_y = \rho_{yx}I_x = \frac{B}{en}I_x = R_H I_x. \quad (3.27)$$

Here, we introduced the Hall resistance  $R_H = B/(en)$ . The carrier density  $n$  can therefore be measured from a transverse measurement alone via the Hall slope  $dR_H/dB = 1/(en)$ , which scales as inverse density. Once the density is known, the mobility  $\mu$  follows from an additional measurement of the longitudinal resistance via  $\mu = (neR_{xx}W/L)^{-1}$ . Note that



the sample dimensions do not enter the expressions for density or Hall-Voltage  $V_H$ ,  $R_H$ , again only true in 2D (in 3D, a thickness would appear). The Hall effect is comparatively large in typical 2D electron gases due to low carrier densities compared to bulk 3D materials:  $R_H \sim 3.1 \text{ k}\Omega/\text{Tesla}$  for  $n \sim 2 \times 10^{-11} \text{ cm}^{-2}$ . The classical Hall effect is very useful for determining carrier concentration and mobility of a given sample.

## 3.4 Quantum Hall Effect

### 3.4.1 Phenomenological Treatment

Due to the (classical) Lorentz-Force  $F = ev \times B$  in a magnetic field  $B$  perpendicular to the 2D electron gas, electrons traveling with velocity  $v$  will move in circles. First we assume that the motion is ballistic, without any scattering. On the circle, the zentrifugal force is equal to the Lorentz force,  $evB = m\omega^2 r$ , and using  $v = \omega r$ , one easily finds the angular frequency  $\omega_c$ , the so-called *cyclotron Frequency* and the radius  $r_c$  of the circle of electron motion, the *cyclotron radius*

$$\omega_c = \frac{eB}{m^*}, \quad r_c = \frac{v}{\omega_c}. \quad (3.28)$$

Note that this corresponds to an energy  $\hbar\omega_c = (1.73 \text{ meV/Tesla}) \cdot B$  which very easily is larger than  $kT$  in many experiments (remember that  $1 \text{ meV}/k_B = 11.6 \text{ K}$ ). The relevant velocity here is again the Fermi velocity  $v_F$ , giving a cyclotron radius of  $r_c \sim (74 \text{ nm Tesla})/B$ . Classically, any radius  $r_c$  would be allowed. Quantum mechanically, however, the circumference must be an integer number  $n$  of Fermi wavelengths  $\lambda_F$  to result in a standing wave:

$$\frac{2\pi r_c}{\lambda_F} = n. \quad (3.29)$$

Using  $r_c = vm^*/(eB)$ ,  $v = \hbar k/m^*$ ,  $k = \sqrt{2m^*E}/\hbar$  and  $\lambda_F = 2\pi/k_F$  one easily finds  $E_n = n\frac{1}{2}\hbar\omega_c$ , in other words, the energy will be quantized in units of the cyclotron frequency. These energy levels  $E_n$  are referred to as *Landau levels*. The correct quantum mechanical treatment will result in a slightly modified quantization condition

$$E_n = (n + 1/2)\hbar\omega_c, \quad (3.30)$$

but this simple argument is giving a qualitatively correct picture. Instead of having a constant density of states as at  $B = 0$ , now the allowed energies are quantized, and the

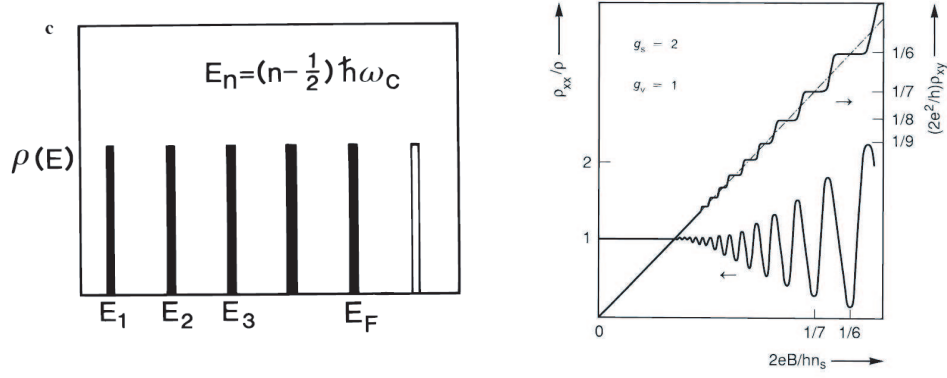


Figure 3.1: left: density of states in a 2DEG in a perpendicular magnetic field. The filled Landau levels are filled bars, empty Landau levels are white bars. Disorder may broaden the Landau levels leading to a nonzero density of states between the peaks (from Beenakker and van Houten (1991)). right: schematic dependence of the normalized longitudinal resistivity  $\rho_{xx}/\rho(0)$  and the Hall Resistance  $R_H = \rho_{xy}$  (normalized to  $h/(2e^2)$ ) on the reciprocal filling factor  $\nu^{-1} = 2eB/(h\nu_s)$  for the case of a single valley with twofold spin degeneracy. Deviations from the classical result are visible at large fields in the form of Shubnikov-deHaas oscillations in  $\rho_{xx}$  and quantized plateaus in  $\rho_{xy}$ . (from Beenakker and van Houten (1991)).

density of states is a series of delta functions spaced by  $\hbar\omega_c$ :

$$\rho_{DOS}(E, B) = N_0 \sum_{n=0}^{\infty} \delta(E - (n + 1/2)\hbar\omega_c) \quad (3.31)$$

with a prefactor  $N_0$  that denotes the number of states per area in each Landau level. From the observation that all zero field states within a range in energy of  $\hbar\omega_c$  are condensed into a single Landau level at  $B \neq 0$  one obtains  $N_0 = \hbar\omega_c \times (m/(\pi\hbar^2)) = 2eB/h$ . As we change magnetic field, the energy and density of states in the Landau levels change. The Landau level filling factor at a given field is defined as

$$\nu = \frac{n}{2eB/h}. \quad (3.32)$$

The filling factor does not have to be an integer, whereas the number  $N$  of Landau levels with  $E_n \leq E_F$  is an integer. As the field is changed, the filling factor will change, and number of occupied Landau may change, too. When the Fermi energy is in the middle of a Landau level ( $\nu = N$ ), states are available for scattering and a maximum in  $\rho_{xx}$  results. When the Fermi energy lies between Landau levels, all Landau levels below  $E_F$  are completely full and above  $E_F$  completely empty. If temperature is small enough to suppress thermal excitation to the next empty Landau level,  $\hbar\omega_c \gg kT$ , then the longitudinal resistance  $\rho_{xx}$  is zero because there is absolutely no phase-space for electron scattering that could cause resistance.

Hence, as the field is ramped up from  $B = 0$  to  $\hbar\omega_c \gg kT$ , oscillations in  $\rho_{xx}$  will occur, with peaks in  $\rho_{xx}$  whenever the Fermi energy is located in a Landau level: the *Shubnikov-deHaas oscillations*. Between two successive peaks at  $B_1$  and  $B_2 > B_1$ , the number of Landau levels has changed by one, yielding

$$\frac{n}{2eB_1/h} - \frac{n}{2eB_2/h} = 1, \quad \rightarrow \quad n = \frac{2e}{h} \frac{1}{(1/B_1) - (1/B_2)} \quad (3.33)$$



Note that the number of occupied Landau levels scales as  $1/B$ , i.e. if we choose  $\beta = (1/B)$  as our variable to plot  $\rho_{xx}$  against, then the peaks will be spaced equidistant with a period  $\Delta\beta = \beta_1 - \beta_2$  and the density will be given by

$$n = \frac{2e}{h} \frac{1}{\Delta\beta} \quad (3.34)$$

Shubnikov-deHaas oscillations can be a very useful tool to determine sample properties such as effective masses, small angle scattering times and subband populations.

The quantization into Landau levels also affects the Hall voltage measurement and results in the quantum Hall effect, namely the occurrence of plateaux in  $R_H$  as a function of magnetic field  $B$  at precisely

$$R_H = \frac{1}{g_s g_v} \frac{h}{e^2} \frac{1}{N} = \frac{h}{2e^2} \frac{1}{N} \quad (3.35)$$

where  $N$  is an integer denoting the number of Landau levels with  $E_n < E_F$ , which changes abruptly as the field is changed. The quantization of the resistance is a more subtle effect that one cannot derive in a few lines.

So far we have neglected disorder causing scattering that can kick electrons off their circular orbits, thus causing broadening of the Landau peaks in the density of states. At a magnetic field where the disorder broadening—given via Heisenberg relation as  $\hbar/\tau_m$ —is much smaller than the Landau level spacing,

$$\hbar\omega_c \gg \hbar/\tau_m, \quad (3.36)$$

the Shubnikov-deHaas oscillations can be resolved. Another way to put this: an electron should be able to go around its circle at least a few times before scattering, i.e.  $\omega_c^{-1} \ll \tau_m$ . Using  $\omega_c = eB/m^*$  and  $\mu = e\tau_m/m^*$ , one obtains:

$$B \gg \mu^{-1} \quad (3.37)$$

The cleaner the sample is, the less disorder broadened are the Landau peaks, an intuitive result. For some of the cleanest samples today ( $\mu \sim 30 \times 10^6 \text{ cm}^2/(\text{Vs})$ ), Shubnikov-deHaas oscillations can be visible at  $B \sim 50 \text{ mT}$ .

Observation of two distinct periods  $\Delta\beta_1$  and  $\Delta\beta_2$  can be an indication of several things:

- two different populated subbands (e. g. in the  $z$  direction) with corresponding partial densities  $n_1 = (2e/h)(1/\Delta\beta_1)$  and  $n_2 = (2e/h)(1/\Delta\beta_2)$ . Often the density of the lower energy subband is significantly larger than the higher energy subband carrier density, giving a fast oscillating component (lower subband, high carrier density, small period in  $1/B$ ) modulated with a much slower envelope (higher subband, low carrier density, large period in  $1/B$ ). However, the mobility in the higher subband might be lower compared to the lower subband, and it might be hard to observe the oscillations from the higher subband.
- spin effects. When the Zeeman energy reaches  $g\mu_B B \gtrsim kT$ , each Landau level will be spin-polarized, giving a doubling of the frequency of the  $\rho_{xx}$  oscillations. (The factor 2 in  $N_0 = 2eB/h$  is due to spin degeneracy). Note that the Zeeman energy ( $g \sim 0.44$ , giving  $E_Z \sim 25 \mu\text{eV}/\text{Tesla}$ ) is much weaker than the Landau quantization energy ( $1.7 \text{ meV}/\text{T}/B$ )

- spin-orbit coupling can cause a (in *GaAs* small) spin splitting of the conduction band, equivalent to two carrier populations with slightly different carrier concentrations. This might appear as the beating of similar frequencies in the Shubnikov-deHaas oscillations.

### 3.4.2 Quantum Mechanical Treatment

We consider electrons in the 2DEG in a constant magnetic field in the  $z$ -direction perpendicular to the plane of the 2DEG in a potential  $U(y)$  in the  $y$ -direction which is uniform in the  $x$ -direction. The Schrödinger equation in the effective mass approximation is

$$\left[ \frac{(i\hbar\nabla + eA)^2}{2m^*} + U(y) \right] \psi(x, y) = E\psi(x, y), \quad (3.38)$$

where we employ the following gauge for the vector potential

$$A = -\hat{x}By \quad \rightarrow \quad A_x = -By \quad \text{and} \quad A_y = 0. \quad (3.39)$$

Obviously this gauge is not unique, and the solutions we might find in another gauge might look very different, though the physics of course must remain the same. This gauge will result in plane waves in the  $x$ -direction. We can rewrite the Schrödinger equation

$$\left[ \frac{(p_x + eBy)^2}{2m^*} + \frac{p_y^2}{2m^*} + U(y) \right] \psi(x, y) = E\psi(x, y) \quad (3.40)$$

where we have used

$$p_x = -i\hbar \frac{\partial}{\partial x} \quad \text{and} \quad p_y = i\hbar \frac{\partial}{\partial y}. \quad (3.41)$$

The solutions for Eq. 3.40 can be expressed in the form of plane waves which we normalize over the length  $L$  of the conductor,

$$\psi(x, y) = \frac{1}{\sqrt{L}} \exp(ikx)\chi(y). \quad (3.42)$$

The transverse function  $\chi(y)$  satisfies the equation

$$\left[ \frac{(\hbar k + eBy)^2}{2m^*} + \frac{p_y^2}{2m^*} + U(y) \right] \chi(y) = E\chi(y) \quad (3.43)$$

We will be interested in the resulting energy spectrum and the transverse eigenfunctions for some combinations of the confining potential  $U$  and the magnetic field  $B$ . A general analytical solution is of course futile, but for a harmonic potential

$$U(y) = \frac{1}{2}m^*\omega_0^2y^2 \quad (3.44)$$

we can write down the solutions. We start with

### 3.4.3 Free electrons in a magnetic field

We set  $U \equiv 0$  and obtain

$$\left[ \frac{p_y^2}{2m^*} + \frac{1}{2} m^* \omega_c^2 (y + y_k)^2 \right] \chi(y) = E \chi(y). \quad (3.45)$$

with

$$y_k = \frac{\hbar k}{eB} \quad \text{and} \quad \omega_c = \frac{eB}{m^*}. \quad (3.46)$$

This is basically the Schrödinger equation of the one-dimensional harmonic oscillator, with a shift  $y_k$ . In an elementary quantum mechanics book, one can look up the solutions

$$\chi_{n,k}(y) = u_n(q + q_k) \quad \text{where} \quad q_{(k)} = \sqrt{m^* \omega_c / \hbar} y_{(k)} \quad (3.47)$$

$$u_n(q) = \exp(-q^2/2) H_n(q) \quad (3.48)$$

$$E(n, k) = \left( n + \frac{1}{2} \right) \hbar \omega_c, \quad n = 0, 1, 2, \dots \quad (3.49)$$

i.e. we just got the Landau-levels, or *magnetic subbands*. The  $H_n(q)$  are the Hermite-polynomials. The first few are:

$$H_0(q) = \frac{1}{\pi^{1/4}} \quad (3.50)$$

$$H_1(q) = \frac{\sqrt{2}q}{\pi^{1/4}} \quad (3.51)$$

$$H_2(q) = \frac{2q^2 - 1}{\sqrt{2}\pi^{1/4}} \quad (3.52)$$

The velocity with which electrons in these states move is given by:

$$v(n, k) = \frac{1}{\hbar} \frac{\partial E(n, k)}{\partial k} = 0. \quad (3.53)$$

Even though the eigenfunctions are plane waves, the group velocity is zero, since the bands have no  $k$ -dependence. This is consistent with our classical picture of electrons moving in circles that don't move in any particular direction. The spatial extent of the wavefunction is approximately

$$\sqrt{\frac{\hbar}{m^* \omega_c}} = \frac{\sqrt{\hbar \omega_c / m^*}}{\omega_c} = \frac{v}{\omega_c}, \quad (3.54)$$

i.e. the same as the radius of the classical orbit (see Eq. 3.28). (One obtains this by setting the ground state ( $n = 0$ ) cyclotron energy  $1/2 \hbar \omega_c$  equal to a kinetic energy  $(1/2) m^* v^2$ , obtaining  $v = \sqrt{\hbar \omega_c / m^*}$ ). As we change the wavevector  $k$  in the longitudinal direction, the wavefunctions shift in the transverse coordinate as given in Eq. 3.47. The wavevector  $k$  is quantized, spaced by  $2\pi/L$ , where  $L$  is the longitudinal size. The corresponding wavefunctions are then spaced by

$$\Delta y_k = \frac{\hbar \Delta k}{eB} = \frac{2\pi \hbar}{eBL} \quad (3.55)$$

along the  $y$ -coordinate. Hence, the total number of states is given by

$$N = 2 \text{ (for spin)} \times \frac{W}{\Delta y_k} = \frac{2eBS}{h} \quad (3.56)$$

where  $S = WL$  is the area. Thus, the quantum mechanical result is in agreement with our heuristic result for the density of states. It can also be seen as one spin degenerate state for each flux quantum through the device area  $S$ .

### 3.5 Electrons Confined in a Constriction

Next, we consider the case of a parabolic confinement potential in the y-direction  $U = 1/2m^*\omega_0^2y^2$  at zero magnetic field. This is the situation of a quantum point contact (QPC). The Schrödinger equation then reads

$$\left[ \frac{\hbar^2 k^2}{2m^*} + \frac{p_y^2}{2m^*} + \frac{1}{2}m^*\omega_0^2y^2 \right] \chi(y) = \chi(y) \quad (3.57)$$

and the solutions are:

$$\chi_{n,k}(y) = u_n(q) \quad \text{where } q = \sqrt{m^*\omega_0/\hbar}y \quad (3.58)$$

$$E(n, k) = \frac{\hbar^2 k^2}{2m^*} + \left( n + \frac{1}{2} \right) \hbar\omega_0, \quad n = 0, 1, 2, \dots \quad (3.59)$$

i.e. we get bands parabolic in  $k$  just as for free electrons, with a second quantization index  $n$  and an energy spacing  $\hbar\omega_0$  due to the parabolic confinement, also called *one-dimensional subbands* or *transverse modes*. This is very similar to the subbands due to the confinement in the z-direction, and analogous to the transverse modes of electromagnetic waveguides. The tighter the confinement is, the larger the subband spacing  $\hbar\omega_0$ . The transverse confinement in a quantum point contact is typically of order of half the Fermi wavelength, or about  $\sim 25$  nm, giving subband spacings of order meV. The velocity of an electron is as in the free electron case given by

$$v(n, k) = \frac{1}{\hbar} \frac{\partial E(n, k)}{\partial k} = \frac{\hbar k}{m^*} \quad (3.60)$$

When a voltage  $V_{sd} = (\mu_s - \mu_d)/e$  is applied between the source and drain reservoirs, the

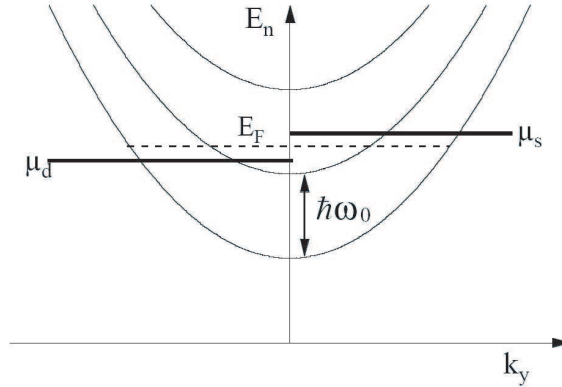


Figure 3.2: Dispersion relation  $E_n(k)$  of one-dimensional subbands formed in a constriction as a function of the longitudinal wavevector  $k$ . Electrons in the source and drain fill the available state up to the chemical potentials  $\mu_s$  and  $\mu_d$ , respectively. When a finite source-drain voltage is applied, a net current results from the uncompensated occupied electron states in the interval between  $\mu_s$  and  $\mu_d$ . (from S. Cronenwett, thesis (2001)).

resulting current  $I$  through the QPC is carried by the uncompensated states in the energy interval defined by  $\mu_s$  and  $\mu_d$ . At zero temperature, the net current is

$$I = e \sum_{n=1}^N \int_{\mu_d}^{\mu_s} dE \frac{1}{2} \rho_n(E) v_n(E) T_n(E), \quad (3.61)$$

where  $\rho_n(E) = 2/\pi(dE_n/dk_x)^{-1}$  is the 1D density of states and  $T_n(E)$  is the transmission probability of the  $n^{\text{th}}$  subband. The factor of  $1/2$  in Eq. 3.61 is to take into account that only half the  $k$  states are filled between  $\mu_s$  and  $\mu_d$ . For small values of  $V_{sd}$ , we can approximate  $T_n(E) = T_n(E_F)$ , independent of energy. The sum over  $n$  counts the number of occupied subbands, where the last occupied subband  $N$  is determined by the condition  $E_N(k_x = 0) < E_F$ . The key to the conductance quantization is that the energy dependence of the 1D density of states exactly cancels that of the velocity, giving the same current for each subband, independent of energy:

$$\begin{aligned} I &= e \sum_{n=1}^N \int_{\mu_d}^{\mu_s} dE \frac{1}{2} \frac{2}{\pi} \left( \frac{\partial E_n}{\partial k_x} \right)^{-1} \frac{1}{\hbar} \frac{\partial E_n}{\partial k_x} T_n(E_F) \\ &= \frac{2e}{h} \sum_{n=1}^N T_n(E_F) \int_{\mu_d}^{\mu_s} dE \\ &= \frac{2e}{h} \sum_{n=1}^N T_n(E_F) eV_{sd}. \end{aligned} \quad (3.62)$$

Using  $I = GV_{sd}$  one then obtains

$$G = \frac{2e^2}{h} \sum_{n=1}^N T_n(E_F) \quad (3.63)$$

and for the case of fully transmitting modes  $\sum_{n=1}^N T_n(E_F) = 1$

$$G = \frac{2e^2}{h} N, \quad (3.64)$$

where each occupied subband contributes  $2e^2/h$  to the conductance through the constriction. The factor 2 is due to spin degeneracy, which can be lifted with a magnetic field, for

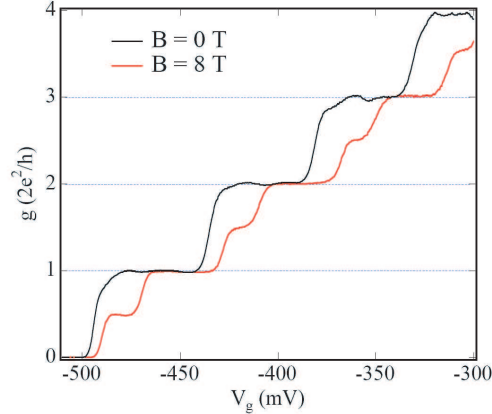


Figure 3.3: Quantized conductance of a QPC at  $B_{\parallel} = 0$  and  $B_{\parallel} = 8$  T. In a large in-plane magnetic field, the spin-degenerate conductance plateaus at multiples of  $2e^2/h$  split into plateaus quantized in units of  $e^2/h$ . (from S. Cronenwett, thesis (2001)).

example with a magnetic field  $B_{\parallel}$  in the plane of the 2DEG (to get (to first order) only a Zeeman energy term). Finite temperature smears what would otherwise be sharp steps in conductance by convolving this zero temperature limit with the derivative of the Fermi-Dirac distribution, resulting in quantized conductance plateaus like those in figure 3.3.

When  $E_Z = g\mu_B B_{\parallel} \gtrsim kT$ , the spin degeneracy is lifted, the subbands then correspond to spin-polarized modes and conductance is quantized in units of  $e^2/h$ . Going from zero conductance onto the first plateau, the transmission probability  $T_1$  is going from zero at  $g = 0$  to one on the first plateau.

### 3.6 Landau-Büttiker Formalism

Equation 3.63 is also known as the 2-terminal Landauer formula. It can also be written in the form

$$G = \frac{2e^2}{h} \sum_{n=1}^N T_n(E_F) = \frac{2e^2}{h} \sum_{n,m=1}^N |t_{mn}|^2 = \frac{2e^2}{h} \text{Tr } \mathbf{t} \mathbf{t}^\dagger \quad (3.65)$$

where now the transmission probabilities  $T_n$  were expressed in terms of the matrix  $\mathbf{t}$  of transmission probability amplitudes from mode  $n$  to mode  $m$ .

$$T_n(E_F) = \sum_{m=1}^N |t_{mn}|^2 \quad (3.66)$$

Equation 3.65 refers to a *two-terminal* resistance measurement, in which the same two contacts or reservoirs are used to drive a current through the system and to measure the voltage drop. More generally, one can consider a multireservoir conductor as in Figure 3.4 to model, for example, *four-terminal* resistance measurements in which the current source and drain are distinct from the voltage probes. This generalization is due to Büttiker. Let  $T_{\alpha \rightarrow \beta}$  denote the total transmission probability from reservoir  $\alpha$  to reservoir  $\beta$ , then

$$T_{\alpha \rightarrow \beta} = \sum_{n=1}^{N_\alpha} \sum_{m=1}^{N_\beta} |t_{\beta\alpha, mn}|^2. \quad (3.67)$$

Here,  $N_\alpha$  is the number of propagating modes in the channel (or “lead”) connected to reservoir  $\alpha$ , which in general may be different from the number  $N_\beta$  in lead  $\beta$ , and  $t_{\beta\alpha, mn}$  is the transmission probability amplitude from mode  $n$  in lead  $\alpha$  to mode  $m$  in lead  $\beta$ . The leads are modeled by ideal electron waveguides, in the sense discussed before for the

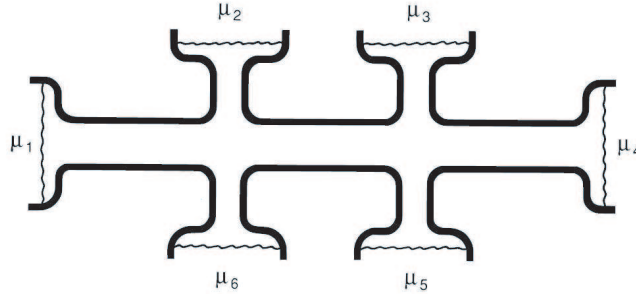


Figure 3.4: Generalized multilead conductor. (from Beenakker and van Houten, thesis (1991)).

case of a quantum point contact, so that the reservoir  $\alpha$  at chemical potential  $\mu_\alpha$  above  $E_F$  injects into lead  $\alpha$  a charge current  $(2e/h)N_\alpha\mu_\alpha$ . A fraction  $T_{\alpha \rightarrow \beta}/N_\alpha$  of that current is transmitted to reservoir  $\beta$ , and a fraction  $T_{\alpha \rightarrow \alpha}/N_\alpha \equiv R_\alpha/N_\alpha$  is reflected back into

reservoir  $\alpha$  before reaching one of the other reservoirs. The net current in  $I_\alpha$  in lead  $\alpha$  is thus given by

$$\frac{h}{2e}I_\alpha = (N_\alpha - R_\alpha)\mu_\alpha - \sum_{\beta(\beta \neq \alpha)} T_{\beta \rightarrow \alpha} \mu_\beta \quad (3.68)$$

The chemical potentials of the reservoirs are related to the currents via a matrix of transmission and reflection coefficients. Current conservation and the requirement that an increase of all the chemical potentials by the same amount should have no effect on the net currents in the leads results in constraints that the set of linear Equations 3.68 has to fulfill. Given additional constraints in the problem one is considering, one can then solve for the unknowns and obtain the four-terminal resistance  $R_{\alpha\beta,\gamma\delta} = V/I$ , in which current flows from lead  $\alpha$  to lead  $\beta$  and a voltage difference  $V$  is measured between leads  $\gamma$  and  $\delta$ . The four-terminal resistance  $R_{\alpha\beta,\gamma\delta} = (\mu_\gamma - \mu_\delta)/(eI)$  is then obtained as a rational function of the transmission and reflection probabilities. This procedure is referred to as *Landauer-Büttiker formalism*. It provides a unified description of electrical transport phenomena in coherent, mesoscopic conductors.

Due to current conservation (unitarity of  $\mathbf{t}$  and time reversal symmetry, one can show that the transmission probabilities have the symmetry

$$t_{\beta\alpha, nm}(B) = t_{\alpha\beta, mn}(-B) \quad \Rightarrow \quad T_{\alpha \rightarrow \beta}(B) = T_{\beta \rightarrow \alpha}(-B) \quad (3.69)$$

As shown by Büttiker, a four terminal *reciprocity relation* for the four-terminal resistances follows:

$$R_{\alpha\beta,\gamma\delta}(B) = R_{\gamma\delta,\alpha\beta}(-B), \quad (3.70)$$

i.e. the resistance is unchanged if current and voltage leads are interchanged with simultaneous reversal of the magnetic field direction. As a special case, it follows that the two-terminal resistance  $R_{\alpha\beta,\alpha\beta}$  is *even* or *symmetric* in  $B$ ,  $G(B) = G(-B)$ . Reciprocity holds only in the linear response regime where the conductor is in or very near equilibrium. In the Landauer-Büttiker formalism, inelastic scattering is assumed to take place only in the reservoirs, which is reasonable if the size of the conductor is much smaller than the phase inelastic scattering or coherence length, often the case in mesoscopic devices.

### 3.7 Confined electrons in nonzero magnetic field

Finally, we consider the combination of both a confining potential and a magnetic field. We again write down the Schödinger equation:

$$\left[ \frac{p_y^2}{2m^*} + \frac{(eBy + \hbar k)^2}{2m^*} + \frac{1}{2}m\omega_0^2 y^2 \right] \chi(y) = E\chi(y) \quad (3.71)$$

It is easy to see that once again, this is basically a one-dimensional Schödinger equation with a parabolic potential and the eigenenergies and eigenfunctions look very similar to the results for electric and magnetic subbands:

$$\chi_{n,k}(y) = u_n \left( q + \frac{\omega_c^2}{\omega_{c0}^2} q_k \right) \quad (3.72)$$

where the electric and magnetic potentials now add in quadrature:

$$\omega_{c0}^2 = \omega_c^2 + \omega_0^2 \quad (3.73)$$

$$q = \sqrt{m^*\omega_{c0}/\hbar} y \quad \text{and} \quad q_k = \sqrt{m^*\omega_{c0}/\hbar} y_k, \quad y_k = \frac{\hbar k}{eB} \quad (3.74)$$

$$E(n, k) = \left( n + \frac{1}{2} \right) \hbar\omega_{c0} + \frac{\hbar^2 k^2}{2m^*} \frac{\omega_0^2}{\omega_{c0}^2}. \quad (3.75)$$

The velocity is then given by

$$v(n, k) = \frac{1}{\hbar} \frac{\partial E(n, k)}{\partial k} = \frac{\hbar k}{m^* \omega_{c0}^2}, \quad (3.76)$$

i.e. for large magnetic fields  $\omega_c \gg \omega_0$  the magnetic field quenches the momentum to zero, while for small magnetic fields  $\omega_c \ll \omega_0$  the dispersion of the confined electron is not

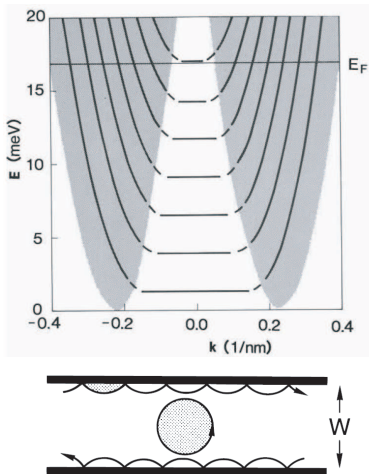


Figure 3.5: Dispersion relation of confined electrons in a magnetic field. Left- and right moving states are spatially separated into chiral edge states.

affected, where we recover the purely electric subbands discussed earlier. The wavefunctions corresponding to a state  $(n, k)$  are centered around  $y = -y_k$ , where

$$y_k = \frac{\hbar k}{eB} \Rightarrow y_k = v(n, k) \frac{\omega_0^2 + \omega_c^2}{\omega_c \omega_0^2} \quad (3.77)$$

one can write the transverse location of the wavefunction in terms of it's velocity. Consider a current carrying state with a given, fixed velocity  $v$ . As the field is increased, it shifts away from the center towards the edge of the sample. In fact, states carrying current along the  $+x$  direction shift to one side of the sample while states carrying current in the other direction shift to the other side of the sample. From a classical point of view, this seems reasonable, since the Lorentz force  $ev \times B$  is opposite for electrons moving in opposite directions. Increasing the magnetic field thus causes a reduction in spatial overlap between forward

and backward propagating states, resulting in a suppression of backscattering that can be very pronounced. The current carrying states will be so called *edge states* that keep bouncing off the same edge and always move towards the same end of the sample, see Figure 3.5.